Inexact Augmented Lagrangian Framework for Non-Convex Optimization

Anonymous Author(s)
Affiliation
Address
email

Abstract

We propose a practical inexact augmented Lagrangian method (iALM) for nonconvex problems with nonlinear constrains. We characterize the total computational complexity of our method subject to a verifiable geometric condition, which is closely related to the Polyak-Lojsiewicz and Mangasarian-Fromowitz conditions.

In particular, when a first-order solver is used for the inner iterates, we prove that iALM finds a first-order stationary point with $\tilde{\mathcal{O}}(1/\epsilon^3)$ calls to the first-order oracle. If, in addition, the problem is smooth and a second-order solver is used for the inner iterates, iALM finds a second-order stationary point with $\tilde{\mathcal{O}}(1/\epsilon^5)$ calls to the second-order oracle. These complexity results match the known theoretical results in the literature with a simple, implementable and versatile algorithm.

We provide numerical evidence on large-scale machine learning problems, including the Burer-Monteiro factorization of semidefinite programs, and a novel nonconvex relaxation of the standard basis pursuit template. We verify our geometric condition in all these examples.

1 Introduction

We study the following nonconvex optimization problem

$$\begin{cases} \min\limits_{x\in\mathbb{R}^d} f(x)+g(x) \\ A(x)=0, \end{cases} \tag{1}$$

where $f:\mathbb{R}^d\to\mathbb{R}$ is a continuously-differentiable nonconvex function, and $A:\mathbb{R}^d\to\mathbb{R}^m$ is a nonlinear operator and $b\in\mathbb{R}^m$. We assume that $g:\mathbb{R}^d\to\mathbb{R}$ is a proximal-friendly (possibly nonsmooth) convex function.

A host of problems in computer science [**? ? ?**], machine learning [**? ?**], and signal processing [**? ?**] naturally fall under the template (1), including max-cut, clustering, generalized eigenvalue decomposition, as well as the quadratic assignment problem (QAP). please add a reference for qap.

To solve (1), this paper proposes an intuitive and easy-to-implement augmented Lagrangian algorithm, and provides its total iteration complexity under an interpretable geometric condition. Before we elaborate on the results, let us first motivate (1) with an application to semidefinite programming (SDP):

Vignette: Burer-Monteiro splitting. A powerful convex relaxation for max-cut, clustering, and several other problems described above is provided by the SDP

$$\begin{cases} \min\limits_{X\in\mathbb{S}^{d\times d}} \langle C,X\rangle \\ B(X)=b,\ X\succeq 0, \end{cases} \tag{2}$$

Submitted to 33rd Conference on Neural Information Processing Systems (NeurIPS 2019). Do not distribute.

where $C \in \mathbb{R}^{d\times d}$, X is a positive semidefinite $d \times d$ matrix, and $B : \mathbb{S}^{d\times d} \to \mathbb{R}^m$ is a linear operator. If the unique-games conjecture is true, SDPs achieve the best approximation for the underlying discrete problem [**?**].

Since d is often large, many first- and second-order methods for solving such SDP's are immediately ruled out, not only due to their high computational complexity, but also due to their storage requirements, which are $\mathcal{O}(d^2)$.

A contemporary challenge in optimization is therefore to solve SDPs using little space and in a scalable fashion. A recent algorithm, namely, homotopy conditional gradient method (HCGM)—based on Linear Minimization Oracles (LMO)—can solve (2) in a small space via sketching [**?**]; however, such LMO-based methods are extremely slow in obtaining accurate solutions.

A key approach for solving (1), dating back to [**?** **?**], is the so-called Burer-Monteiro (BM) factorization $X = UU^\top$, where $U \in \mathbb{R}^{d\times r}$ and r is selected according to the guidelines in [**?** **?**], which are shown to be optimal [**?**]. This factorization does not introduce any extraneous local minima [**?**]. Moreover, [**?**] established the connection between local minima of factorized problem 3 and global optimum for 2. might have to double check this

This factorization leads to the nonconvex problem

$$\begin{cases} \min\limits_{U\in\mathbb{R}^{d\times r}} \langle C, UU^\top\rangle \\ B(UU^\top) = b, \end{cases} \tag{3}$$

which can be easily written in the form of (1). To solve (3), the inexact Augmented Lagrangian Method (iALM) is widely used [**?** **?** **?**], due to its cheap per iteration cost and its empirical success. Every (outer) iteration of iALM calls a solver to solve an intermediate augmented Lagrangian subproblem to near stationarity, and the user is free in the choice of this solver, which could use first-order, such as the proximal gradient descent [**?**], or second-order information, such as an BFGS [**?**].

Unlike its convex counterpart [**?** **?** **?**], the convergence rate and the complexity of iALM for (3) are not well-understood, see Section 5 for a review of the related literature. Indeed, addressing this important theoretical gap is one of the contributions of our work.

Summary of contributions:

∘ Our framework is future-proof in the sense that we obtain the convergence rate of iALM for (1) with an arbitrary solver for finding first- and second-order stationary points.

∘ We investigate the effect of using different solvers for augmented Lagrangian subproblems and provide overall iteration complexity bounds for finding first- and second-order stationary points of (1). Our complexity bounds match the best theoretical results in optimization, see Section 5.

∘ We propose a geometric condition that simplifies the algorithmic analysis for iALM, and clarify its connection to well-known Polyak-Lojasiewicz and Mangasarian-Fromovitz conditions. please add citations for these conditions here. We also verify this condition for key problems in Section 6. how about the KL condition spars'19 reviewers pointed out?

Roadmap. Section 2 collects the main tools and our notation. We present the iALM in Section 3 and obtain its convergence rate to first- and second-order stationary points in Section 4, alongside their iteration complexities. We provide a comprehensive review of the literature and highlight our key differences in Section 5. Section 6 presents the numerical evidence and comparisons with the state-of-the-art techniques.

2 Preliminaries

Notation. We use the notation $\langle\cdot,\cdot\rangle$ and $\|\cdot\|$ for the standard inner product and the norm on $\mathbb{R}^d$. For matrices, $\|\cdot\|$ and $\|\cdot\|_F$ denote the spectral and the Frobenius norms, respectively. For the convex function $g : \mathbb{R}^d \to \mathbb{R}$, the subdifferential set at $x \in \mathbb{R}^d$ is denoted by $\partial g(x)$ and we will occasionally use the notation $\partial g(x)/\beta = \{z/\beta : z \in \partial g(x)\}$. When presenting iteration complexity results, we often use $\widetilde{O}(\cdot)$ which suppresses the logarithmic dependencies.

We use the indicator function $\delta_{\mathcal{X}} : \mathbb{R}^d \to \mathbb{R}$ of a set $\mathcal{X} \subset \mathbb{R}^d$, which takes x to

$$\delta_{\mathcal{X}}(x) = \begin{cases} 0 & x \in \mathcal{X} \\ \infty & x \notin \mathcal{X}. \end{cases} \tag{4}$$

The distance function from a point x to $\mathcal{X}$ is denoted by $\operatorname{dist}(x, \mathcal{X}) = \min_{z \in \mathcal{X}} \|x - z\|$. For integers $k_0 \leq k_1$, we denote $[k_0 : k_1] = \{k_0, \ldots, k_1\}$.

For an operator $A : \mathbb{R}^d \to \mathbb{R}^m$ with components $\{A_i\}_{i=1}^m$, we let $DA(x) \in \mathbb{R}^{m \times d}$ denote the Jacobian of A, where the ith row of $DA(x)$ is the gradient vector $\nabla A_i(x) \in \mathbb{R}^d$.

Smoothness. We require $f : \mathbb{R}^d \to \mathbb{R}$ and $A : \mathbb{R}^d \to \mathbb{R}^m$ to be smooth, namely, there exist $\lambda_f, \lambda_A \geq 0$ such that

$$\begin{aligned} \|\nabla f(x) - \nabla f(x')\| &\leq \lambda_f \|x - x'\|, \\ \|DA(x) - DA(x')\| &\leq \lambda_A \|x - x'\|, \end{aligned} \tag{5}$$

for every $x, x' \in \mathbb{R}^d$.

Augmented Lagrangian method (ALM). ALM is a classical algorithm, which first appeared in [**? ?**] and extensively studied afterwards in [**? ?**]. For solving (1), ALM suggests solving the problem

$$\min_x \max_y \; \mathcal{L}_\beta(x, y) + g(x), \tag{6}$$

where, for penalty weight $\beta > 0$, $\mathcal{L}_\beta$ is the corresponding augmented Lagrangian, defined as

$$\mathcal{L}_\beta(x, y) := f(x) + \langle A(x), y \rangle + \frac{\beta}{2} \|A(x)\|^2. \tag{7}$$

The minimax formulation in (6) naturally suggests the following algorithm for solving (1). For dual step sizes $\{\sigma_k\}_k$, consider the iterations

$$\begin{aligned} x_{k+1} &\in \operatorname*{argmin}_x \; \mathcal{L}_\beta(x, y_k) + g(x), \\ y_{k+1} &= y_k + \sigma_k A(x_{k+1}). \end{aligned} \tag{8}$$

However, computing x_{k+1} above requires solving the nonconvex problem (8) to optimality, which is typically intractable. Instead, it is often easier to find an approximate first- or second-order stationary point of (8).

Hence, we argue that by gradually improving the stationarity precision and increasing the penalty weight β above, we can reach a stationary point of the main problem in (1), as detailed in Section 3.

Optimality conditions. First-order necessary optimality conditions for (1) are well-studied. Indeed, $x \in \mathbb{R}^d$ is a first-order stationary point of (1) if there exists $y \in \mathbb{R}^m$ such that

$$\begin{cases} -\nabla f(x) - DA(x)^\top y \in \partial g(x) \\ A(x) = 0, \end{cases} \tag{9}$$

where $DA(x)$ is the Jacobian of A at x. Recalling (7), we observe that (9) is equivalent to

$$\begin{cases} -\nabla_x \mathcal{L}_\beta(x, y) \in \partial g(x) \\ A(x) = 0, \end{cases} \tag{10}$$

which is in turn the necessary optimality condition for (6). mfs: check approx. optimality conditions, how they apply in this setting. Inspired by this, we say that x is an (ϵ_f, β) first-order stationary point of (6) if there exists a $y \in \mathbb{R}^m$ such that

$$\begin{cases} \operatorname{dist}(-\nabla_x \mathcal{L}_\beta(x, y), \partial g(x)) \leq \epsilon_f \\ \|A(x)\| \leq \epsilon_f, \end{cases} \tag{11}$$

for $\epsilon_f \geq 0$. In light of (11), a suitable metric for evaluating the stationarity of a pair $(x, y) \in \mathbb{R}^d \times \mathbb{R}^m$ is

$$\operatorname{dist}\left(-\nabla_x \mathcal{L}_\beta(x, y), \partial g(x)\right) + \|A(x)\|, \tag{12}$$

which we use as the first-order stopping criterion. As an example, for a convex set $\mathcal{X} \subset \mathbb{R}^d$, suppose that $g = \delta_{\mathcal{X}}$ is the indicator function on $\mathcal{X}$. Let also $T_{\mathcal{X}}(x) \subseteq \mathbb{R}^d$ denote the tangent cone to $\mathcal{X}$ at x, and with $P_{T_{\mathcal{X}}(x)} : \mathbb{R}^d \to \mathbb{R}^d$ we denote the orthogonal projection onto this tangent cone. Then, for $u \in \mathbb{R}^d$, it is not difficult to verify that

$$\operatorname{dist}(u, \partial g(x)) = \|P_{T_{\mathcal{X}}(x)}(u)\|. \tag{13}$$

When $g = 0$, a first-order stationary point $x \in \mathbb{R}^d$ of (1) is also second-order stationary if

$$\lambda_{\min}(\nabla_{xx}\mathcal{L}_\beta(x, y)) \geq 0, \tag{14}$$

where $\nabla_{xx}\mathcal{L}_\beta$ is the Hessian of $\mathcal{L}_\beta$ with respect to x, and $\lambda_{\min}(\cdot)$ returns the smallest eigenvalue of its argument. Analogously, x is an $(\epsilon_f, \epsilon_s, \beta)$ second-order stationary point if, in addition to (11), it holds that

$$\lambda_{\min}(\nabla_{xx}\mathcal{L}_\beta(x, y)) \geq -\epsilon_s, \tag{15}$$

for $\epsilon_s \geq 0$. Naturally, for second-order stationarity, we use $\lambda_{\min}(\nabla_{xx}\mathcal{L}_\beta(x, y))$ as the stopping criterion.

Smoothness lemma. This next result controls the smoothness of $\mathcal{L}_\beta(\cdot, y)$ for a fixed y. The proof is standard but nevertheless is included in Appendix C for completeness.

Lemma 2.1 (smoothness) *For fixed $y \in \mathbb{R}^m$ and $\rho, \rho' \geq 0$, it holds that*

$$\|\nabla_x\mathcal{L}_\beta(x, y) - \nabla_x\mathcal{L}_\beta(x', y)\| \leq \lambda_\beta\|x - x'\|, \tag{16}$$

for every $x, x' \in \{x'' : \|x''\| \leq \rho, \|A(x'')\| \leq \rho'\}$, where

$$\begin{aligned}\lambda_\beta &\leq \lambda_f + \sqrt{m}\lambda_A\|y\| + (\sqrt{m}\lambda_A\rho' + d\lambda_A'^2)\beta \\ &=: \lambda_f + \sqrt{m}\lambda_A\|y\| + \lambda''(A, \rho, \rho')\beta.\end{aligned} \tag{17}$$

Above, λ_f, λ_A were defined in (5) and

$$\lambda_A' := \max_{\|x\| \leq \rho} \|DA(x)\|. \tag{18}$$

3 Algorithm

To solve the equivalent formulation of (1) presented in (6), we propose the inexact ALM (iALM), detailed in Algorithm 1.

At the k^{th} iteration, Step 2 of Algorithm 1 calls a solver that finds an approximate stationary point of the augmented Lagrangian $\mathcal{L}_{\beta_k}(\cdot, y_k)$ with the accuracy of ϵ_{k+1}, and this accuracy gradually increases in a controlled fashion.

The increasing sequence of penalty weights $\{\beta_k\}_k$ and the dual update (Steps 4 and 5) are responsible for continuously enforcing the constraints in (1). The appropriate choice for $\{\beta_k\}_k$ will be specified in Sections 4.1 and 4.2.

As we will see in the convergence analysis, the particular choice of the dual step sizes $\{\sigma_k\}_k$ in Algorithm 1 ensures that the dual variable y_k remains bounded, see [**?**] for a precedent in the ALM literature where a similar choice for σ_k is considered.

4 Convergence Rate

In this section, we detail the convergence rate of Algorithm 1 for finding first-order and second-order stationary points, along with total iteration complexity results. All the proofs are deferred to Appendix A. Theorem 4.1 below characterizes the convergence rate of Algorithm 1 for finding stationary points in terms of the number of outer iterations.

Algorithm 1 Inexact ALM for solving (1)

Input: Non-decreasing, positive, unbounded sequence $\{\beta_k\}_{k\geq 1}$, stopping thresholds $\tau_f > 0$ and $\tau_s > 0$.

Initialization: Initial primal variable $x_1 \in \mathbb{R}^d$, initial dual variable $y_0 \in \mathbb{R}^m$, initial dual step size $\sigma_1 > 0$.

for $k = 1, 2, \ldots$ **do**

1. **(Update tolerance)** $\epsilon_{k+1} = 1/\beta_k$.
2. **(Inexact primal solution)** Obtain $x_{k+1} \in \mathbb{R}^d$ such that

$$\operatorname{dist}(-\nabla_x \mathcal{L}_{\beta_k}(x_{k+1}, y_k), \partial g(x_{k+1})) \leq \epsilon_{k+1}$$

for first-order stationarity

$$\lambda_{\min}(\nabla_{xx} \mathcal{L}_{\beta_k}(x_{k+1}, y_k)) \geq -\epsilon_{k+1}$$

for second-order-stationarity, if $g = 0$ in (1).

3. **(Update dual step size)**

$$\sigma_{k+1} = \sigma_1 \min\Big(\frac{\|A(x_1)\| \log^2 2}{\|A(x_{k+1})\|(k+1)\log^2(k+2)}, 1\Big).$$

4. **(Dual ascent)** $y_{k+1} = y_k + \sigma_{k+1} A(x_{k+1})$.
5. **(Stopping criterion)** If

$$\operatorname{dist}(-\nabla_x \mathcal{L}_{\beta_k}(x_{k+1}), \partial g(x_{k+1})) + \|A(x_{k+1})\| \leq \tau_f,$$

for first-order stationarity and if also $\lambda_{\min}(\nabla_{xx} \mathcal{L}_{\beta_k}(x_{k+1}, y_k)) \geq -\tau_s$ for second-order stationarity, then quit and return x_{k+1} as an (approximate) stationary point of (1).

end for

Theorem 4.1 (convergence rate) *Let $\rho := \sup_{k\in[K]} \|x\|$.[1] Suppose that f and A satisfy (5) and let*

$$\lambda'_f = \max_{\|x\|\leq\rho} \|\nabla f(x)\|, \;\; \lambda'_A = \max_{\|x\|\leq\rho} \|DA(x)\|, \tag{19}$$

be the (restricted) Lipschitz constants of f and A, respectively. For integers $2 \leq k_0 \leq k_1$, consider the interval $K = [k_0 : k_1]$, and let $\{x_k\}_{k\in K}$ be the output sequence of Algorithm 1 on the interval K.[2] For $\nu > 0$, assume that

$$\nu \|A(x_k)\| \leq \operatorname{dist}\left(-DA(x_k)^\top A(x_k), \frac{\partial g(x_k)}{\beta_{k-1}}\right), \tag{20}$$

for every $k \in K$. We consider two cases:

- *If a first-order solver is used in Step 2, then x_k is an $(\epsilon_{k,f}, \beta_k)$ first-order stationary point of (1) with*

$$\begin{aligned}\epsilon_{k,f} &= \frac{1}{\beta_{k-1}}\left(\frac{2(\lambda'_f + \lambda'_A y_{\max})(1 + \lambda'_A \sigma_k)}{\nu} + 1\right) \\ &=: \frac{Q(f, g, A, \sigma_1)}{\beta_{k-1}},\end{aligned} \tag{21}$$

for every $k \in K$, where the expression for $y_{\max}(x_1, y_0, \sigma_1)$ is given in (41) due to the limited space.

[1] If necessary, to ensure that $\rho < \infty$, one can add a small factor of $\|x\|^2$ to $\mathcal{L}_\beta$ in (7). Then it is easy to verify that the iterates of Algorithm 1 remain bounded, provided that the penalty weight β is large enough, $\sup_x \|\nabla f(x)\|/\|x\| < \infty$ and $\sup_x \|A(x)\| < \infty$.

[2] The choice of $k_1 = \infty$ is valid here too.

- *If a second-order solver is used in Step 2, then x_k is an $(\epsilon_{k,f}, \epsilon_{k,s}, \beta_k)$ second-order stationary point of (1) with $\epsilon_{k,s}$ specified above and with*

$$\begin{aligned}\epsilon_{k,s} &= \epsilon_{k-1} + \sigma_k\sqrt{m}\lambda_A \frac{2\lambda'_f + 2\lambda'_A y_{\max}}{\nu\beta_{k-1}} \\ &= \frac{\nu + \sigma_k\sqrt{m}\lambda_A 2\lambda'_f + 2\lambda'_A y_{\max}}{\nu\beta_{k-1}} =: \frac{Q'(f, g, A, \sigma_1)}{\beta_{k-1}}.\end{aligned} \tag{22}$$

Loosely speaking, Theorem 4.1 states that Algorithm 1 converges to a (first- or second-) order stationary point of (1) at the rate of $1/\beta_k$. A few remarks are in order.

Regularity. The key geometric condition in Theorem 4.1 is (20) which, broadly speaking, ensures that the primal updates of Algorithm 1 reduce the feasibility gap as the penalty weight β_k grows. We will verify this condition for several examples in Section 6.

This condition is closely related to those in the existing literature. In the special case where $g = 0$ in (1), it is easy to verify that (20) reduces to the Polyak-Lojasiewicz (PL) condition for minimizing $\|A(x)\|^2$ [**?**]. PL condition itself is a special case of Kurdyka-Lojasiewicz with $\theta = 1/2$, see [**?** , Definition 1.1]. When $g = 0$, it is also easy to see that (20) is weaker than the Mangasarian-Fromovitz condition in nonlinear optimization [**?**].

By its definition, we may think of (20) as a local condition, which should hold within a neighborhood of the constraint set $\{x : A(x) = 0\}$ rather than everywhere in $\mathbb{R}^d$. There is a constant complexity algorithm in [**?**] to reach this so-called "information zone", which supplements Theorem 4.1.

Moreover, in contrast to most conditions in the nonconvex optimization literature, such as [**?**], the condition in (20) appears to be easier to verify, as we see in Section 6.

AE: Fatih, I think you had added the following two references to our response for icml. Could you discuss their relevance here? [2] Rockafellar, Lagrange Multipliers and Optimality, 1993 [3] Bertsekas, On penalty and multiplier methods for constrained minimization. 1996

AE: the spars review talks about the "Pong-Li" work. Fatih, do you know what is that?

Penalty method. A classical algorithm to solve (1) is the penalty method, which is characterized by the absence of the dual variable ($y = 0$) in (7). Indeed, ALM can be interpreted as an adaptive penalty or smoothing method with a variable center as determined by the dual variable. It is worth noting that, with same proof technique, one can establish the same convergence rate of Theorem 4.1 for the penalty method. However, while both methods have the same convergence rate in theory, iALM outperforms the penalty method in practice by virtue of its variable center and has been excluded from this presentation.

Computational complexity. Theorem 4.1 allows us to specify the number of (outer) iterations that Algorithm 1 requires to reach a near-stationary point of problem (1) with a prescribed precision and, in particular, specifies the number of calls made to the solver in Step 2. In this sense, Theorem 4.1 does not fully capture the computational complexity of Algorithm 1, as it does not take into account the computational cost of the solver in Step 2.

To better understand the total iteration complexity of Algorithm 1, we consider two scenarios in the following. In the first scenario, we take the solver in Step 2 to be the Accelerated Proximal Gradient Method (APGM), a well-known first-order algorithm [**?**]. In the second scenario, we will use the second-order trust region method developed in [**?**].

4.1 First-Order Optimality

Let us first consider the case where the solver in Step 2 is is the first-order algorithm APGM, described in detail in [**?**]. At a high level, APGM makes use of $\nabla_x \mathcal{L}_\beta(x, y)$, the proximal operator prox_g and classical Nesterov acceleration for the iterates [**?**] to reach first-order stationarity for the first update in (8). Suppose that $g = \delta_{\mathcal{X}}$ is the indicator function on a bounded convex set $\mathcal{X} \subset \mathbb{R}^d$ and let

$$\rho' = \max_{x \in \mathcal{X}} \|x\|, \tag{23}$$

be the radius of a ball centered at the origin that includes $\mathcal{X}$. Then, adapting the results in [**?**] to our setup, APGM reaches x_k in Step 2 of Algorithm 1 after

$$\mathcal{O}\left(\frac{\lambda_{\beta_k}^2 \rho'^2}{\epsilon_{k+1}}\right) \tag{24}$$

(inner) iterations, where λ_{β_k} denotes the Lipschitz constant of $\nabla_x \mathcal{L}_{\beta_k}(x, y)$, bounded in (17). For the clarity of the presentation, we have used a looser bound in (24) compared to [**?**]. Using (24), we derive the following corollary, describing the total iteration complexity of Algorithm 1 in terms of the number calls made to the first-order oracle in APGM.

Corollary 4.2 *For $b > 1$, let $\beta_k = b^k$ for every k. If we use APGM from [**?**] for Step 2 of Algorithm 1, the algorithm finds an (ϵ_f, β_k) first-order stationary point, after T calls to the first-order oracle, where*

$$T = \mathcal{O}\left(\frac{Q^3 \rho'^2}{\epsilon^3} \log_b\left(\frac{Q}{\epsilon}\right)\right) = \tilde{\mathcal{O}}\left(\frac{Q^3 \rho'^2}{\epsilon^3}\right). \tag{25}$$

For Algorithm 1 to reach a near-stationary point with an accuracy of ϵ_f in the sense of (11) and with the lowest computational cost, we therefore need to perform only one iteration of Algorithm 1, with β_1 specified as a function of ϵ_f by (21) in Theorem 4.1. In general, however, the constants in (21) are unknown and this approach is thus not feasible. Instead, the homotopy approach taken by Algorithm 1 ensures achieving the desired accuracy by gradually increasing the penalty weight.[3] This homotopy approach increases the computational cost of Algorithm 1 only by a factor logarithmic in the ϵ_f, as detailed in the proof of Corollary 4.2.

4.2 Second-Order Optimality

Let us now consider the second-order optimality case where the solver in Step 2 is the the trust region method developed in [**?**]. Trust region method minimizes quadratic approximation of the function within a dynamically updated trust-region radius. Second-order trust region method that we consider in this section makes use of Hessian (or an approximation of Hessian) of the augmented Lagrangian in addition to first order oracles.

As shown in [**?**], finding approximate second-order stationary points of convex-constrained problems is in general NP-hard. For this reason, we focus in this section on the special case of (1) with $g = 0$.

Let us compute the total computational complexity of Algorithm 1 with the trust region method in Step 2, in terms of the number of calls made to the second-order oracle. By adapting the result in [**?**] to our setup, we find that the number of (inner) iterations required in Step 2 of Algorithm 1 to produce x_{k+1} is

$$\mathcal{O}\left(\frac{\lambda_{\beta_k,H}^2 (\mathcal{L}_{\beta_k}(x_1, y) - \min_x \mathcal{L}_{\beta_k}(x, y))}{\epsilon_k^3}\right), \tag{26}$$

where $\lambda_{\beta,H}$ is the Lipschitz constant of the Hessian of the augmented Lagrangian, which is of the order of β, as can be proven similar to Lemma 2.1 and x_1 is the initial iterate of the given outer loop. In [**?**], the term $\mathcal{L}_\beta(x_1, y) - \min_x \mathcal{L}_\beta(x, y)$ is bounded by a constant independent of ϵ. We assume a uniform bound for this quantity $\forall \beta_k$, instead of for one value of β_k as in [**?**]. Using (26) and Theorem 4.1, we arrive at the following:

Corollary 4.3 *For $b > 1$, let $\beta_k = b^k$ for every k. We assume that*

$$\mathcal{L}_\beta(x_1, y) - \min_x \mathcal{L}_\beta(x, y) \leq L_u, \ \ \forall \beta. \tag{27}$$

*If we use the trust region method from [**?**] for Step 2 of Algorithm 1, the algorithm finds an ϵ-second-order stationary point of (1) in T calls to the second-order oracle where*

$$T \leq \mathcal{O}\left(\frac{L_u Q'^5}{\epsilon^5} \log_b\left(\frac{Q'}{\epsilon}\right)\right) = \widetilde{\mathcal{O}}\left(\frac{L_u Q'^5}{\epsilon^5}\right). \tag{28}$$

Before closing this section, we note that the remark after Corollary 4.2 applies here as well.

[3] In this context, homotopy loosely corresponds to the gradual enforcement of the constraints by increasing the penalty weight.

5 Related Work

ALM has a long history in the optimization literature, dating back to [**?** **?**]. In the special case of (1) with a convex function f and a linear operator A, standard, inexact and linearized versions of ALM have been extensively studied [**?** **?** **?** **?**].

Classical works on ALM focused on the general template of (1) with nonconvex f and nonlinear A, with arguably stronger assumptions and required exact solutions to the subproblems of the form (8), which appear in Step 2 of Algorithm 1, see for instance [**?**].

A similar analysis was conducted in [**?**] for the general template of (1). The authors considered inexact ALM and proved convergence rates for the outer iterates, under specific assumptions on the initialization of the dual variable. However, unlike our results, the authors did not analyze how to solve the subproblems inexactly and they did not provide total complexity results and verifiable conditions.

Problem (1) with similar assumptions to us is also studied in [**?**] and [**?**] for first-order and second-order stationarity, respectively, with explicit iteration complexity analysis. As we have mentioned in Section 4, our iteration complexity results matches these theoretical algorithms with a simpler algorithm and a simpler analysis. In addition, these algorithms require setting final accuracies since they utilize this information in the algorithm. In contrast to [**?** **?**], Algorithm 1 does not set accuracies a priori.

[**?**] also considers the same template (1) for first-order stationarity with a penalty-type method instead of ALM. Even though the authors show $\mathcal{O}(1/\epsilon^2)$ complexity, this result is obtained by assuming that the penalty parameter remains bounded. We note that such an assumption can also be used to match our complexity results.

[**?**] studies the general template (1) with specific assumptions involving local error bound conditions for the (1). These conditions are studied in detail in [**?**], but their validity for general SDPs (2) has never been established. This work also lacks the total iteration complexity analysis presented here.

Another work [**?**] focused on solving (1) by adapting the primal-dual method of Chambolle and Pock [**?**]. The authors proved the convergence of the method and provided convergence rate by imposing error bound conditions on the objective function that do not hold for standard SDPs.

[**?** **?**] is the first work that proposes the splitting $X = UU^\top$ for solving SDPs of the form (2). Following these works, the literature on Burer-Monteiro (BM) splitting for the large part focused on using ALM for solving the reformulated problem (3).

However, this approach has a few drawbacks: First, it requires exact solutions in Step 2 of Algorithm 1 in theory, which in practice is replaced with inexact solutions. Second, their results only establish convergence without providing the rates. In this sense, our work provides a theoretical understanding of the BM splitting with inexact solutions to Step 2 of Algorithm 1 and complete iteration complexities.

[**?** **?**] are among the earliest efforts to show convergence rates for BM splitting, focusing on the special case of SDPs without any linear constraints. For these specific problems, they prove the convergence of gradient descent to global optima with convergence rates, assuming favorable initialization. These results, however, do not apply to general SDPs of the form (2) where the difficulty arises due to the linear constraints.

[**?**] focused on the quadratic penalty formulation of (1), namely,

$$\min_{X \succeq 0} \langle C, X \rangle + \frac{\mu}{2} \|B(x) - b\|^2, \tag{29}$$

which after BM splitting becomes

$$\min_{U \in \mathbb{R}^{d \times r}} \langle C, UU^\top \rangle + \frac{\mu}{2} \|B(UU^\top) - b\|^2, \tag{30}$$

for which they study the optimality of the second-order stationary points. These results are for establishing a connection between the stationary points of (30) and global optima of (29). In contrast, we focus on the relation of the stationary points of (6) to the constrained problem (1).

Another popular method for solving SDPs are due to [**?** **?** **?**], focusing on the case where the constraints in (1) can be written as a Riemannian manifold after BM splitting. In this case, the authors

apply the Riemannian gradient descent and Riemannian trust region methods for obtaining first- and second-order stationary points, respectively. They obtain $\mathcal{O}(1/\epsilon^2)$ complexity for finding first-order stationary points and $\mathcal{O}(1/\epsilon^3)$ complexity for finding second-order stationary points.

While these complexities appear better than ours, the smooth manifold requirement in these works is indeed restrictive. In particular, this requirement holds for max-cut and generalized eigenvalue problems, but it is not satisfied for other important SDPs such as quadratic programming (QAP), optimal power flow and clustering with general affine constraints. In addition, as noted in [**?**], per iteration cost of their method for max-cut problem is an astronomical $\mathcal{O}(d^6)$.

Lastly, there also exists a line of work for solving SDPs in their original convex formulation, in a storage efficient way [**?** **?** **?**]. These works have global optimality guarantees by their virtue of directly solving the convex formulation. On the downside, these works require the use of eigenvalue routines and exhibit significantly slower convergence as compared to nonconvex approaches [**?**].

6 Numerical Evidence

We first begin with a caveat: It is known that quasi-Newton methods, such as BFGS and lBFGS, might not converge for nonconvex problems [**?** **?**]. For this reason, we have used the trust region method as the second-order solver in our analysis in Section 4, which is well-studied for nonconvex problems [**?**]. Empirically, however, BFGS and lBGFS are extremely successful and we have therefore opted for those solvers in this section since the subroutine does not affect Theorem 4.1 as long as the subsolver performs well in practice.

6.1 Clustering

Given data points $\{z_i\}_{i=1}^n$, the entries of the corresponding Euclidean distance matrix $D \in \mathbb{R}^{nxn}$ are $D_{i,j} = \|z_i - z_j\|^2$. Clustering is then the problem of finding a co-association matrix $Y \in \mathbb{R}^{n\times n}$ such that $Y_{ij} = 1$ if points z_i and z_j are within the same cluster and $Y_{ij} = 0$ otherwise. In [**?**], the authors provide a SDP relaxation of the clustering problem, specified as

$$\begin{cases} \min\limits_{Y\in\mathbb{R}^{nxn}} \text{tr}(DY) \\ Y\mathbf{1} = \mathbf{1},\ \text{tr}(Y) = s,\ Y \succeq 0,\ Y \geq 0, \end{cases} \tag{31}$$

where s is the number of clusters and Y is both positive semidefinite and has nonnegative entries. Standard SDP solvers do not scale well with the number of data points n, since they often require projection onto the semidefinite cone with the complexity of $\mathcal{O}(n^3)$. We instead use the Burer-Monteiro factorization to solve (31), sacrificing convexity to reduce the computational complexity. More specifically, we solve the program

$$\begin{cases} \min\limits_{V\in\mathbb{R}^{nxr}} \text{tr}(DVV^\top) \\ VV^\top\mathbf{1} = \mathbf{1},\ \ \|V\|_F^2 \leq s,\ \ V \geq 0, \end{cases} \tag{32}$$

where $\mathbf{1} \in \mathbb{R}^n$ is the vector of all ones. Note that $Y \geq 0$ in (31) is replaced above by the much stronger but easier-to-enforce constraint $V \geq 0$ in (32), see [**?**] for the reasoning behind this relaxation. Now, we can cast (32) as an instance of (1). Indeed, for every $i \leq n$, let $x_i \in \mathbb{R}^r$ denote the ith row of V. We next form $x \in \mathbb{R}^d$ with $d = nr$ by expanding the factorized variable V, namely,

$$x = [x_1^\top, \cdots, x_n^\top]^\top \in \mathbb{R}^d,$$

and then set

$$f(x) = \sum_{i,j=1}^n D_{i,j} \langle x_i, x_j \rangle, \qquad g = \delta_C,$$

$$A(x) = [x_1^\top \sum_{j=1}^n x_j - 1, \cdots, x_n^\top \sum_{j=1}^n x_j - 1]^\top, \tag{33}$$

where C is the intersection of the positive orthant in $\mathbb{R}^d$ with the Euclidean ball of radius $\sqrt{s}$. In Appendix D, we somewhat informally verify that Theorem 4.1 applies to (1) with f, g, A specified above.

In our simulations, we use two different solvers for Step 2 of Algorithm 1, namely, APGM and lBFGS. APGM is a solver for nonconvex problems of the form (8) with convergence guarantees to first-order stationarity, as discussed in Section 4. lBFGS is a limited-memory version of BFGS algorithm in [**?**] that approximately leverages the second-order information of the problem. We compare our approach against the following convex methods:

- HCGM: Homotopy-based Conditional Gradient Method in [**?**] which directly solves (31).
- SDPNAL+: A second-order augmented Lagrangian method for solving SDP's with nonnegativity constraints [**?**].

As for the dataset, our experimental setup is similar to that described by [**?**]. We use the publicly-available fashion-MNIST data in [**?**], which is released as a possible replacement for the MNIST handwritten digits. Each data point is a 28×28 gray-scale image, associated with a label from ten classes, labeled from 0 to 9. First, we extract the meaningful features from this dataset using a simple two-layer neural network with a sigmoid activation function. Then, we apply this neural network to 1000 test samples from the same dataset, which gives us a vector of length 10 for each data point, where each entry represents the posterior probability for each class. Then, we form the ℓ_2 distance matrix D from these probability vectors. The results are depicted in Figure 1. We implemented 3 algorithms on MATLAB and used the software package for SDPNAL+ which contains mex files. It is predictable that the performance of our nonconvex approach would also improve by using mex files.

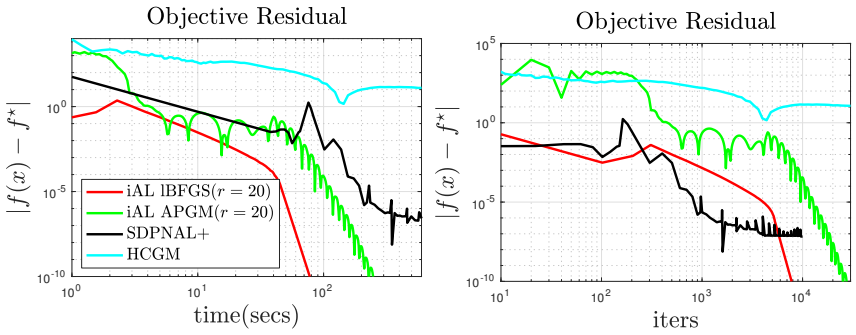

Figure 1: Convergence of different algorithms for clustering with fashion-MNIST dataset. Here, we set the rank as $r = 20$ for the nonconvex approaches. The solution rank for the template (31) is the number of clusters s [**?** , Theorem 1]. However, as discussed in [**?**], setting rank $r > s$ leads more accurate reconstruction at the expense of speed, hence our choice of $r = 20$.

6.2 Basis Pursuit

Basis Pursuit (BP) finds sparsest solutions of an under-determined system of linear equations, namely,

$$\begin{cases} \min_z \|z\|_1 \\ Bz = b, \end{cases} \tag{34}$$

where $B \in \mathbb{R}^{n\times d}$ and $b \in \mathbb{R}^n$. BP has found many applications in machine learning, statistics and signal processing [**?** **?** **?**]. A plethora of primal-dual convex optimization algorithms are available in the literature to solve BP, including [**?** **?**]. There also exists a line of work [**?**] that handles sparse regression via regularization with ℓ_1 norm.

Here, we take a different approach and cast (34) as an instance of (1). Note that any $z \in \mathbb{R}^d$ can be decomposed as $z = z^+ - z^-$, where $z^+, z^- \in \mathbb{R}^d$ are the positive and negative parts of z, respectively. Then consider the change of variables $z^+ = u_1^{\circ 2}$ and $z^- = u_2^{\circ 2} \in \mathbb{R}^d$, where $\circ$ denotes element-wise power. Next, we concatenate u_1 and u_2 as $x := [u_1^\top, u_2^\top]^\top \in \mathbb{R}^{2d}$ and define $\overline{B} := [B, -B] \in \mathbb{R}^{n\times 2d}$. Then, (34) is equivalent to (1) with

$$\begin{aligned} f(x) =& \|x\|^2, \quad g(x) = 0 \\ A(x) =& \overline{B}x^{\circ 2} - b. \end{aligned} \tag{35}$$

In Appendix E, we verify with minimal detail that Theorem 4.1 indeed applies to (1) with the above f, A.

We draw the entries of B independently from a zero-mean and unit-variance Gaussian distribution. For a fixed sparsity level k, the support of $z_* \in \mathbb{R}^d$ and its nonzero amplitudes are also drawn from the standard Gaussian distribution. Then the measurement vector is created as $b = Bz + \epsilon$, where ϵ is the noise vector with entries drawn independently from the zero-mean Gaussian distribution with variance $\sigma^2 = 10^{-6}$.

AE: the image sizes throughout the paper are inconsistent which is not nice. The font size in Fig 3 is also very different from the rest of the paper which is not nice. please change.

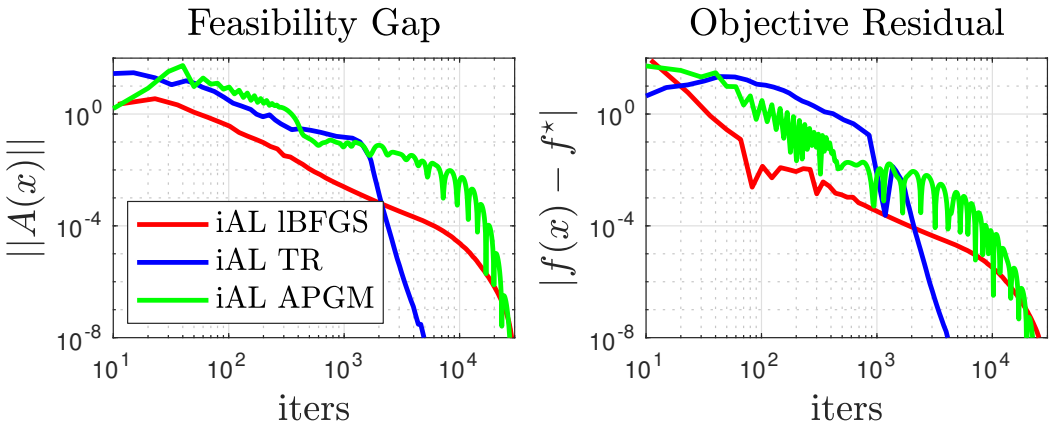

Figure 2: Convergence with different subsolvers for the aforementioned nonconvex relaxation.

Figure 2 compiles our results for the proposed relaxation. It is, indeed, interesting to see that these type of nonconvex relaxations gives the solution of convex one and first order methods succeed.

Discussion: The true potential of our reformulation is in dealing with more structured norms rather than ℓ_1, where computing the proximal operator is often intractable. One such case is the latent group lasso norm [**?**], defined as

$$\|z\|_\Omega = \sum_{i=1}^{I} \|z_{\Omega_i}\|,$$

where $\{\Omega_i\}_{i=1}^I$ are (not necessarily disjoint) index sets of $\{1, \cdots, d\}$. Although not studied here, we believe that the nonconvex framework presented in this paper can serve to solve more complicated problems, such as the latent group lasso. We leave this research direction for future work.

References

A Proof of Theorem 4.1

For every $k \geq 2$, recall from (7) and Step 2 of Algorithm 1 that x_k satisfies

$$\begin{aligned}&\operatorname{dist}(-\nabla f(x_k) - DA(x_k)^\top y_{k-1} \\ &\qquad - \beta_{k-1} DA(x_k)^\top A(x_k), \partial g(x_k)) \\ &= \operatorname{dist}(-\nabla_x \mathcal{L}_{\beta_{k-1}}(x_k, y_{k-1}), \partial g(x_k)) \leq \epsilon_k. \end{aligned} \tag{36}$$

With an application of the triangle inequality, it follows that

$$\begin{aligned}&\operatorname{dist}(-\beta_{k-1} DA(x_k)^\top A(x_k), \partial g(x_k)) \\ &\qquad \leq \|\nabla f(x_k)\| + \|DA(x_k)^\top y_{k-1}\| + \epsilon_k, \end{aligned} \tag{37}$$

which in turn implies that

$$\begin{aligned}&\operatorname{dist}(-DA(x_k)^\top A(x_k), \partial g(x_k)/\beta_{k-1}) \\ &\leq \frac{\|\nabla f(x_k)\|}{\beta_{k-1}} + \frac{\|DA(x_k)^\top y_{k-1}\|}{\beta_{k-1}} + \frac{\epsilon_k}{\beta_{k-1}} \\ &\leq \frac{\lambda_f' + \lambda_A' \|y_{k-1}\| + \epsilon_k}{\beta_{k-1}}, \end{aligned} \tag{38}$$

where λ_f', λ_A' were defined in (19). We next translate (38) into a bound on the feasibility gap $\|A(x_k)\|$. Using the regularity condition (20), the left-hand side of (38) can be bounded below as

$$\operatorname{dist}(-DA(x_k)^\top A(x_k), \partial g(x_k)/\beta_{k-1}) \geq \nu \|A(x_k)\|. \qquad \text{(see (20))} \tag{39}$$

By substituting (39) back into (38), we find that

$$\|A(x_k)\| \leq \frac{\lambda_f' + \lambda_A' \|y_{k-1}\| + \epsilon_k}{\nu \beta_{k-1}}. \tag{40}$$

In words, the feasibility gap is directly controlled by the dual sequence $\{y_k\}_k$. We next establish that the dual sequence is bounded. Indeed, for every $k \in K$, note that

$$\begin{aligned}\|y_k\| &= \|y_0 + \sum_{i=1}^{k} \sigma_i A(x_i)\| \quad \text{(Step 5 of Algorithm 1)} \\ &\leq \|y_0\| + \sum_{i=1}^{k} \sigma_i \|A(x_i)\| \qquad \text{(triangle inequality)} \\ &\leq \|y_0\| + \sum_{i=1}^{k} \frac{\|A(x_1)\| \log^2 2}{k \log^2(k+1)} \quad \text{(Step 4)} \\ &\leq \|y_0\| + c\|A(x_1)\| \log^2 2 =: y_{\max}, \end{aligned} \tag{41}$$

where

$$c \geq \sum_{i=1}^{\infty} \frac{1}{k \log^2(k+1)}. \tag{42}$$

Substituting (41) back into (40), we reach

$$\begin{aligned}\|A(x_k)\| &\leq \frac{\lambda_f' + \lambda_A' y_{\max} + \epsilon_k}{\nu \beta_{k-1}} \\ &\leq \frac{2\lambda_f' + 2\lambda_A' y_{\max}}{\nu \beta_{k-1}}, \end{aligned} \tag{43}$$

where the second line above holds if k_0 is large enough, which would in turn guarantees that $\epsilon_k = 1/\beta_{k-1}$ is sufficiently small since $\{\beta_k\}_k$ is increasing and unbounded. It remains to control

the first term in (12). To that end, after recalling Step 2 of Algorithm 1 and applying the triangle inequality, we can write that

$$\begin{aligned}&\operatorname{dist}(-\nabla_x \mathcal{L}_{\beta_{k-1}}(x_k, y_k), \partial g(x_k))\\ &\leq \operatorname{dist}(-\nabla_x \mathcal{L}_{\beta_{k-1}}(x_k, y_{k-1}), \partial g(x_k))\\ &+ \|\nabla_x \mathcal{L}_{\beta_{k-1}}(x_k, y_k) - \nabla_x \mathcal{L}_{\beta_{k-1}}(x_k, y_{k-1})\|. \end{aligned} \tag{44}$$

The first term on the right-hand side above is bounded by ϵ_k, by Step 5 of Algorithm 1. For the second term on the right-hand side of (44), we write that

$$\begin{aligned}&\|\nabla_x \mathcal{L}_{\beta_{k-1}}(x_k, y_k) - \nabla_x \mathcal{L}_{\beta_{k-1}}(x_k, y_{k-1})\|\\ &= \|DA(x_k)^\top (y_k - y_{k-1})\| \qquad \text{(see (7))}\\ &\leq \lambda'_A \|y_k - y_{k-1}\| \qquad \text{(see (19))}\\ &= \lambda'_A \sigma_k \|A(x_k)\| \qquad \text{(see Step 5 of Algorithm 1)}\\ &\leq \frac{2\lambda'_A \sigma_k}{\nu \beta_{k-1}} (\lambda'_f + \lambda'_A y_{\max}). \qquad \text{(see (43))} \end{aligned} \tag{45}$$

By combining (44,45), we find that

$$\begin{aligned}&\operatorname{dist}(\nabla_x \mathcal{L}_{\beta_{k-1}}(x_k, y_k), \partial g(x_k))\\ &\leq \frac{2\lambda'_A \sigma_k}{\nu \beta_{k-1}} (\lambda'_f + \lambda'_A y_{\max}) + \epsilon_k. \end{aligned} \tag{46}$$

By combining (43,46), we find that

$$\begin{aligned}&\operatorname{dist}(-\nabla_x \mathcal{L}_{\beta_{k-1}}(x_k, y_k), \partial g(x_k)) + \|A(x_k)\|\\ &\leq \left(\frac{2\lambda'_A \sigma_k}{\nu \beta_{k-1}} (\lambda'_f + \lambda'_A y_{\max}) + \epsilon_k \right)\\ &\quad + 2 \left(\frac{\lambda'_f + \lambda'_A y_{\max}}{\nu \beta_{k-1}} \right). \end{aligned} \tag{47}$$

Applying $\sigma_k \leq \sigma_1$, we find that

$$\begin{aligned}&\operatorname{dist}(-\nabla_x \mathcal{L}_{\beta_{k-1}}(x_k, y_k), \partial g(x_k)) + \|A(x_k)\|\\ &\leq \frac{2\lambda'_A \sigma_1 + 2}{\nu \beta_{k-1}} (\lambda'_f + \lambda'_A y_{\max}) + \epsilon_k. \end{aligned} \tag{48}$$

For the second part of the theorem, we use the Weyl's inequality and Step 5 of Algorithm 1 to write

$$\begin{aligned}&\lambda_{\min}(\nabla_{xx} \mathcal{L}_{\beta_{k-1}}(x_k, y_{k-1})) \geq \lambda_{\min}(\nabla_{xx} \mathcal{L}_{\beta_{k-1}}(x_k, y_k))\\ &- \sigma_k \| \sum_{i=1}^m A_i(x_k) \nabla^2 A_i(x_k)\|. \end{aligned} \tag{49}$$

The first term on the right-hand side is lower bounded by $-\epsilon_{k-1}$ by Step 2 of Algorithm 1. We next bound the second term on the right-hand side above as

$$\begin{aligned}&\sigma_k \| \sum_{i=1}^m A_i(x_k) \nabla^2 A_i(x_k)\|\\ &\leq \sigma_k \sqrt{m} \max_i \|A_i(x_k)\| \|\nabla^2 A_i(x_k)\|\\ &\leq \sigma_k \sqrt{m} \lambda_A \frac{2\lambda'_f + 2\lambda'_A y_{\max}}{\nu \beta_{k-1}}, \end{aligned}$$

where the last inequality is due to (5,43). Plugging into (49) gives

$$\begin{aligned}&\lambda_{\min}(\nabla_{xx} \mathcal{L}_{\beta_{k-1}}(x_k, y_{k-1}))\\ &\geq -\epsilon_{k-1} - \sigma_k \sqrt{m} \lambda_A \frac{2\lambda'_f + 2\lambda'_A y_{\max}}{\nu \beta_{k-1}}, \end{aligned}$$

which completes the proof of Theorem 4.1.

B Proof of Corollary 4.2

Let K denote the number of (outer) iterations of Algorithm 1 and let ϵ_f denote the desired accuracy of Algorithm 1, see (11). Recalling Theorem 4.1, we can then write that

$$\epsilon_f = \frac{Q}{\beta_K}, \tag{50}$$

or, equivalently, $\beta_K = Q/\epsilon_f$. We now count the number of total (inner) iterations T of Algorithm 1 to reach the accuracy ϵ_f. From (17) and for sufficiently large k, recall that $\lambda_{\beta_k} \leq \lambda'' \beta_k$ is the smoothness parameter of the augmented Lagrangian. Then, from (24) ad by summing over the outer iterations, we bound the total number of (inner) iterations of Algorithm 1 as

$$\begin{aligned}
T &= \sum_{k=1}^{K} \mathcal{O}\left(\frac{\lambda_{\beta_{k-1}}^2 \rho'^2}{\epsilon_k}\right) \\
&= \sum_{k=1}^{K} \mathcal{O}\left(\beta_{k-1}^3 \rho'^2\right) \qquad \text{(Step 1 of Algorithm 1)} \\
&\leq \mathcal{O}\left(K \beta_{K-1}^3 \rho'^2\right) \qquad (\{\beta_k\}_k \text{ is increasing}) \\
&\leq \mathcal{O}\left(\frac{K Q^3 \rho'^2}{\epsilon_f^3}\right). \qquad \text{(see (50))}
\end{aligned} \tag{51}$$

In addition, if we specify $\beta_k = b^k$ for all k, we can further refine T. Indeed,

$$\beta_K = b^K \implies K = \log_b\left(\frac{Q}{\epsilon_f}\right), \tag{52}$$

which, after substituting into (51) gives the final bound in Corollary 4.2.

C Proof of Lemma 2.1

Note that

$$\mathcal{L}_\beta(x, y) = f(x) + \sum_{i=1}^{m} y_i A_i(x) + \frac{\beta}{2} \sum_{i=1}^{m} (A_i(x))^2, \tag{53}$$

which implies that

$$\begin{aligned}
&\nabla_x \mathcal{L}_\beta(x, y) \\
&= \nabla f(x) + \sum_{i=1}^{m} y_i \nabla A_i(x) + \frac{\beta}{2} \sum_{i=1}^{m} A_i(x) \nabla A_i(x) \\
&= \nabla f(x) + DA(x)^\top y + \beta DA(x)^\top A(x),
\end{aligned} \tag{54}$$

where $DA(x)$ is the Jacobian of A at x. By taking another derivative with respect to x, we reach

$$\begin{aligned}
\nabla_x^2 \mathcal{L}_\beta(x, y) = \nabla^2 f(x) &+ \sum_{i=1}^{m} \left(y_i + \beta A_i(x)\right) \nabla^2 A_i(x) \\
&+ \beta \sum_{i=1}^{m} \nabla A_i(x) \nabla A_i(x)^\top.
\end{aligned} \tag{55}$$

It follows that

$$\begin{aligned}
&\|\nabla_x^2 \mathcal{L}_\beta(x, y)\| \\
&\leq \|\nabla^2 f(x)\| + \max_i \|\nabla^2 A_i(x)\| \left(\|y\|_1 + \beta \|A(x)\|_1\right) \\
&\quad + \beta \sum_{i=1}^{m} \|\nabla A_i(x)\|^2 \\
&\leq \lambda_h + \sqrt{m} \lambda_A \left(\|y\| + \beta \|A(x)\|\right) + \beta \|DA(x)\|_F^2.
\end{aligned} \tag{56}$$

For every x such that $\|x\| \le \rho$ and $\|A(x)\| \le \rho$, we conclude that

$$\|\nabla_x^2 \mathcal{L}_\beta(x,y)\| \le \lambda_f + \sqrt{m}\lambda_A\left(\|y\| + \beta\rho'\right) + \beta \max_{\|x\|\le\rho} \|DA(x)\|_F^2, \tag{57}$$

which completes the proof of Lemma 2.1.

D Clustering

We only verify the condition in (20). Note that

$$A(x) = VV^\top \mathbf{1} - \mathbf{1}, \tag{58}$$

$$\begin{aligned} DA(x) &= \begin{bmatrix} w_{1,1}x_1^\top & \cdots & w_{1,n}x_1^\top \\ \vdots & & \\ w_{n,1}x_n^\top & \cdots & w_{n,n}1x_n^\top \end{bmatrix} \\ &= \begin{bmatrix} V & \cdots & V \end{bmatrix} + \begin{bmatrix} x_1^\top & & \\ & \ddots & \\ & & x_n^\top \end{bmatrix}, \end{aligned} \tag{59}$$

where $w_{i.i} = 2$ and $w_{i,j} = 1$ for $i \neq j$. In the last line above, n copies of V appear and the last matrix above is block-diagonal. For x_k, define V_k as in the example and let $x_{k,i}$ be the ith row of V_k. Consequently,

$$\begin{aligned} DA(x_k)^\top A(x_k) = &\begin{bmatrix} (V_k^\top V_k - I_n)V_k^\top \mathbf{1} \\ \vdots \\ (V_k^\top V_k - I_n)V_k^\top \mathbf{1} \end{bmatrix} \\ &+ \begin{bmatrix} x_{k,1}(V_kV_k^\top \mathbf{1} - \mathbf{1})_1 \\ \vdots \\ x_{k,n}(V_kV_k^\top \mathbf{1} - \mathbf{1})_n \end{bmatrix}, \end{aligned} \tag{60}$$

where $I_n \in \mathbb{R}^{n\times n}$ is the identity matrix. Let us make a number of simplifying assumptions. First, we assume that $\|x_k\| < \sqrt{s}$, which can be easily enforced in the iterates. Under this assumption, it follows that

$$(\partial g(x_k))_i = \begin{cases} 0 & (x_k)_i > 0 \\ \{a : a \le 0\} & (x_k)_i = 0, \end{cases} \qquad i \le d. \tag{61}$$

Second, we assume that V_k has nearly orthonormal columns, namely, $V_k^\top V_k \approx I_n$. This can also be easily enforced in each iterate of Algorithm 1 and naturally corresponds to well-separated clusters. While a more fine-tuned argument can remove these assumptions, they will help us simplify the presentation here. Under these assumptions, the (squared) right-hand side of (20) becomes

$$\begin{aligned} &\operatorname{dist}\left(-DA(x_k)^\top A(x_k), \frac{\partial g(x_k)}{\beta_{k-1}}\right)^2 \\ &= \left\| \left(-DA(x_k)^\top A(x_k)\right)_+ \right\|^2 \qquad (a_+ = \max(a,0)) \\ &= \left\| \begin{bmatrix} x_{k,1}(V_kV_k^\top \mathbf{1} - \mathbf{1})_1 \\ \vdots \\ x_{k,n}(V_kV_k^\top \mathbf{1} - \mathbf{1})_n \end{bmatrix} \right\|^2 \qquad (x_k \in C \Rightarrow x_k \ge 0) \\ &= \sum_{i=1}^n \|x_{k,i}\|^2 (V_kV_k^\top \mathbf{1} - \mathbf{1})_i^2 \\ &\ge \min_i \|x_{k,i}\|^2 \cdot \sum_{i=1}^n (V_kV_k^\top \mathbf{1} - \mathbf{1})_i^2 \\ &= \min_i \|x_{k,i}\|^2 \cdot \|V_kV_k^\top \mathbf{1} - \mathbf{1}\|^2. \end{aligned} \tag{62}$$

Given a prescribed ν, ensuring $\|x_{k,i}\| \geq \nu$ guarantees (20). This requirement corresponds again to well-separated clusters. When the clusters are sufficiently separated and the algorithm is initialized close enough to the constraint set, there is indeed no need to separately enforce this condition. In practice, often n exceeds the number of true clusters and a more fine-tuned analysis is required to establish (20) by restricting the argument to a particular subspace of $\mathbb{R}^n$.

E Basis Pursuit

We only verify the regularity condition in (20) for (1) with f, A, g specified in (35). Note that

$$DA(x) = 2\overline{B}\text{diag}(x), \tag{63}$$

where $\text{diag}(x) \in \mathbb{R}^{2d\times 2d}$ is the diagonal matrix formed by x. The left-hand side of (20) then reads as

$$\begin{aligned}
&\text{dist}\left(-DA(x_k)^\top A(x_k), \frac{\partial g(x_k)}{\beta_{k-1}}\right)\\
&= \text{dist}\left(-DA(x_k)^\top A(x_k), \{0\}\right) \qquad (g \equiv 0)\\
&= \|DA(x_k)^\top A(x_k)\|\\
&= 2\|\text{diag}(x_k)\overline{B}^\top(\overline{B}x_k^{\circ 2} - b)\|. \qquad \text{(see (63))}
\end{aligned} \tag{64}$$

To bound the last line above, let x_* be a solution of (1) and note that $\overline{B}x_*^{\circ 2} = b$ by definition. Let also $z_k, z_* \in \mathbb{R}^d$ denote the vectors corresponding to x_k, x_*. Corresponding to x_k, also define $u_{k,1}, u_{k,2}$ naturally and let $|z_k| = u_{k,1}^{\circ 2} + u_{k,2}^{\circ 2} \in \mathbb{R}^d$ be the amplitudes of z_k. To simplify matters, let us assume also that B is full-rank. We then rewrite the last line of (64) as

$$\begin{aligned}
&\|\text{diag}(x_k)\overline{B}^\top(\overline{B}x_k^{\circ 2} - b)\|^2\\
&= \|\text{diag}(x_k)\overline{B}^\top\overline{B}(x_k^{\circ 2} - x_*^{\circ 2})\|^2 \qquad (\overline{B}x_*^{\circ 2} = b)\\
&= \|\text{diag}(x_k)\overline{B}^\top B(x_k - x_*)\|^2\\
&= \|\text{diag}(u_{k,1})B^\top B(z_k - z_*)\|^2\\
&\quad + \|\text{diag}(u_{k,2})B^\top B(z_k - z_*)\|^2\\
&= \|\text{diag}(u_{k,1}^{\circ 2} + u_{k,2}^{\circ 2})B^\top B(z_k - z_*)\|^2\\
&= \|\text{diag}(|z_k|)B^\top B(z_k - z_*)\|^2\\
&\geq \eta_n(B\text{diag}(|z_k|))^2\|B(z_k - z_*)\|^2\\
&= \eta_n(B\text{diag}(|z_k|))^2\|Bz_k - b\|^2 \qquad (Bz_* = \overline{B}x_*^{\circ 2} = b)\\
&\geq \min_{|T|=n} \eta_n(B_T)\cdot |z_{k,(n)}|^2\|Bz_k - b\|^2,
\end{aligned} \tag{65}$$

where $\eta_n(\cdot)$ returns the nth largest singular value of its argument. In the last line above, B_T is the restriction of B to the columns indexed by T of size n. Moreover, $z_{k,(n)}$ is the nth largest entry of z in magnitude. Given a prescribed ν, (20) therefore holds if

$$|z_{k,(n)}| \geq \sqrt{\frac{\nu}{\min_{|T|=n}\eta_n(B_T)\cdot\|Bz_k - b\|^2}}, \tag{66}$$

for every iteration k. If Algorithm 1 is initialized close enough to the solution z^*, there will be no need to directly enforce this condition.

Discussion The true potential of the reformulation of BP in (35) is in dealing with more structured norms than ℓ_1, where computing the proximal operator is often intractable. One such case is the latent group lasso norm [**?**], defined as

$$\|z\|_\Omega = \sum_{i=1}^{I}\|z_{\Omega_i}\|,$$

where $\{\Omega_i\}_{i=1}^I$ are (not necessarily disjoint) index sets of $\{1,\cdots,d\}$. Although not studied here, we believe that the non-convex framework presented in this paper can serve to solve more complicated problems, such as the latent group lasso. We leave this research direction for future work.

E.1 ℓ_∞ Denoising with a Generative Prior

The authors of [**?**] have proposed to project onto the range of a Generative Adversarial network (GAN) [**?**], as a way to defend against adversarial examples. For a given noisy observation $x^* + \eta$, they consider a projection in the ℓ_2 norm. We instead propose to use our augmented Lagrangian method to denoise in the ℓ_∞ norm, a much harder task:

$$\begin{array}{ll} \min\limits_{x,z} & \|x^* + \eta - x\|_\infty \\ \text{s.t.} & x = G(z). \end{array} \tag{67}$$

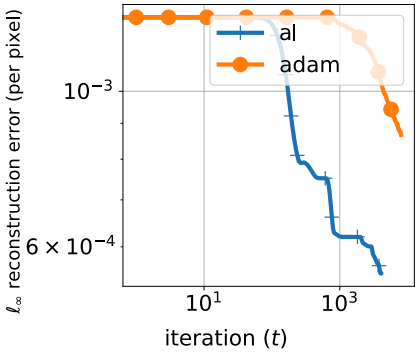

Figure 3: Augmented Lagrangian vs Adam for ℓ_∞ denoising (left). ℓ_2 vs ℓ_∞ denoising as defense against adversarial examples

We use a pretrained generator for the MNIST dataset, given by a standard deconvolutional neural network architecture. We compare the succesful optimizer Adam against our method. Our algorithm involves two forward/backward passes through the network, as oposed to Adam that requires only one. For this reason we let our algorithm run for 4000 iterations, and Adam for 8000 iterations. For a particular example, we plot the objective value vs iteration count in figure E.1. Our method successfully minimizes the objective value, while Adam does not succeed.

E.2 Generalized Eigenvalue Problem

Generalized eigenvalue problem has extensive applications in machine learning, statistics and data analysis [**?**]. The well-known nonconvex formulation of the problem is [**?**].

$$\begin{cases} \min\limits_{x \in \mathbb{R}^n} x^\top C x \\ x^\top B x = 1, \end{cases} \tag{68}$$

where $B, C \in \mathbb{R}^{n \times n}$ are symmetric matrices and B is positive definite, i.e. $B \succ 0$. The generalized eigenvector computation is equivalent to performing principal component analysis (PCA) of C in the norm B. Moreover, it is also equivalent to computing the top eigenvector of symmetric matrix $S = B^{-1/2} C B^{1-2}$ and multiplying the resulting vector by $B^{-1/2}$. However, for sufficiently large n, computing $B^{-1/2}$ is extremely expensive. The natural convex sdp relaxation for (68) involves lifting $Y = xx^\top$ and removes the non-convex $\text{rank}(Y) = 1$ constraint,

$$\begin{cases} \min\limits_{Y \in \mathbb{R}^{n \times n}} \text{tr}(CY) \\ \text{tr}(BY) = 1, \quad X \succeq 0. \end{cases} \tag{69}$$

Here, we solve (68) because it directly fits into our template with,

$$\begin{aligned} f(x) =& x^\top C x, \quad g(x) = 0 \\ A(x) =& x^\top B x - 1. \end{aligned} \tag{70}$$

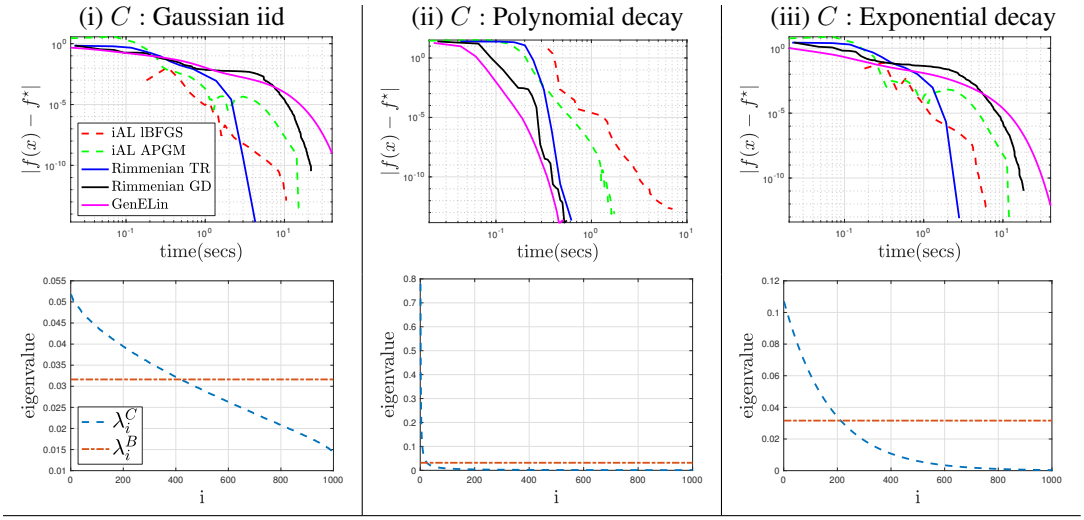

Figure 4: *(Top)* Objective convergence for calculating top generalized eigenvalue and eigenvector of B and C. *(Bottom)* Eigenvalue structure of the matrices. For (i),(ii) and (iii), C is positive semidefinite; for (iv), (v) and (vi), C contains negative eigenvalues. [(i): Generated by taking symmetric part of iid Gaussian matrix. (ii): Generated by randomly rotating diag$(1^{-p}, 2^{-p}, \cdots, 1000^{-p})(p = 1)$. (iii): Generated by randomly rotating diag$(10^{-p}, 10^{-2p}, \cdots, 10^{-1000p})(p = 0.0025)$.]

We compare our approach against 3 different methods. Manifold based Riemannian gradient descent and Riemannian trust region methods in[**?**] and generalized eigenvector via linear system solver (abbrevated as. GenELin) in [**?**]. We have used Manopt software package in [**?**] for the manifold based methods. For GenELin, we have utilized Matlab's backslash operator as the linear solver. The results are compiled in Figure 4.